Porosity of spacer-filled channels in spiral-wound membrane systems

Quantification methods and impact on hydraulic characterization

Siddiqui, A; Lehmann, S; Haaksman, V.; Ogier, J.; Schellenberg, Carsten; van Loosdrecht, M. C.M.; Kruithof, J. C.; Vrouwenvelder, J. S.

DOI
10.1016/j.watres.2017.04.034

Publication date
2017

Document Version
Final published version

Published in
Water Research

Citation (APA)
Siddiqui, A., Lehmann, S., Haaksman, V., Ogier, J., Schellenberg, C., van Loosdrecht, M. C. M., Kruithof, J. C., & Vrouwenvelder, J. S. (2017). Porosity of spacer-filled channels in spiral-wound membrane systems: Quantification methods and impact on hydraulic characterization. *Water Research*, *119*, 304-311. https://doi.org/10.1016/j.watres.2017.04.034

Water Research 119 (2017) 304–311

Contents lists available at ScienceDirect

Water Research

journal homepage: www.elsevier.com/locate/watres

Porosity of spacer-filled channels in spiral-wound membrane systems: Quantification methods and impact on hydraulic characterization

A. Siddiqui [a], S. Lehmann [b], V. Haaksman [c], J. Ogier [b], C. Schellenberg [b], M.C.M. van Loosdrecht [c], J.C. Kruithof [d], J.S. Vrouwenvelder [a, c, d, *]

[a] King Abdullah University of Science and Technology (KAUST), Water Desalination and Reuse Center (WDRC), Division of Biological and Environmental Science and Engineering (BESE), Thuwal 23955-6900, Saudi Arabia
[b] LANXESS BU Liquid Purification Technologies, R&D Membranes, 06803 Bitterfeld-Wolfen, Germany
[c] Department of Biotechnology, Faculty of Applied Sciences, Delft University of Technology, Van der Maasweg 9, 2629 HZ Delft, The Netherlands
[d] Wetsus, European Centre of Excellence for Sustainable Water Technology, Oostergoweg 9, 8911 MA Leeuwarden, The Netherlands

ARTICLE INFO

Article history:
Received 10 January 2017
Received in revised form
6 April 2017
Accepted 10 April 2017
Available online 13 April 2017

Keywords:
Porosity measurement methods
Spacer-filled channel
Feed spacer geometry modification
Linear flow velocity
Pressure drop

ABSTRACT

The porosity of spacer-filled feed channels influences the hydrodynamics of spiral-wound membrane systems and impacts the overall performance of the system. Therefore, an exact measurement and a detailed understanding of the impact of the feed channel porosity is required to understand and improve the hydrodynamics of spiral-wound membrane systems applied for desalination and wastewater reuse. The objectives of this study were to assess the accuracy of porosity measurement techniques for feed spacers differing in geometry and thickness and the consequences of using an inaccurate method on hydrodynamic predictions, which may affect permeate production. Six techniques were applied to measure the porosity namely, three volumetric techniques based on spacer strand count together with a cuboidal (SC), cylindrical (VCC) and ellipsoidal volume calculation (VCE) and three independent techniques based on volume displacement (VD), weight and density (WD) and computed tomography (CT) scanning. The CT method was introduced as an alternative for the other five already existing and applied methods in practice.

Six feed spacers used for the porosity measurement differed in filament thickness, angle between the filaments and mesh-size. The results of the studies showed differences between the porosities, measured by the six methods. The results of the microscopic techniques SC, VCC and VCE deviated significantly from measurements by VD, WD and CT, which showed similar porosity values for all spacer types.

Depending on the maximum deviation of the porosity measurement techniques from −6% to +6%, (i) the linear velocity deviations were −5.6% and +6.4% respectively and (ii) the pressure drop deviations were −31% and +43% respectively, illustrating the importance of an accurate porosity measurement. Because of the accuracy and standard deviation, the VD and WD method should be applied for the porosity determination of spacer-filled channels, while the CT method is recommended for numerical modelling purposes. The porosity has a linear relationship with the flow velocity and a superlinear effect on the pressure drop. Accurate porosity data are essential to evaluate feed spacer performance in spiral-wound membrane systems. Porosity of spacer-filled feed channels has a strong impact on membrane performance and biofouling impact.

1. Introduction

1.1. General

Biofouling is a serious problem in nanofiltration (NF) and reserve osmosis (RO) membrane systems, since pre-treatment cannot completely prevent biomass accumulation (Vrouwenvelder et al., 2008). Biofouling is the amount of biomass

* Corresponding author. King Abdullah University of Science and Technology (KAUST), Water Desalination and Reuse Center (WDRC), Division of Biological and Environmental Science and Engineering (BESE), Thuwal 23955-6900, Saudi Arabia.
E-mail addresses: Amber.Siddiqui@kaust.edu.sa (A. Siddiqui), Stefan.Lehmann@lanxess.com (S. Lehmann), V.A.Haaksman@tudelft.nl (V. Haaksman), Julien.Ogier@lanxess.com (J. Ogier), Carsten.Schellenberg@lanxess.com (C. Schellenberg), M.C.M.vanloosdrecht@tudelft.nl (M.C.M. van Loosdrecht), Joop.Kruithof@wetsus.nl (J.C. Kruithof), Johannes.Vrouwenvelder@kaust.edu.sa, J.S.Vrouwenvelder@tudelft.nl (J.S. Vrouwenvelder).

http://dx.doi.org/10.1016/j.watres.2017.04.034
0043-1354/

causing an unacceptable decline in membrane performance (Flemming, 2002). In recent years, many strategies have been implemented to overcome biofouling (Al Ashhab et al., 2014; Baker and Dudley, 1998; Ben-Sasson et al., 2014; Habimana et al., 2014; Ridgway et al., 1983; Ridgway and Flemming, 1996; Schneider et al., 2005; Schwinge et al., 2004; Tasaka et al., 1994; Vrouwenvelder et al., 2008; Vrouwenvelder and Van der Kooij, 2001; Ying et al., 2013). Some strategies have focussed on reducing the impact of biomass accumulation on the performance of spiral-wound membrane systems by modifying the hydraulics of the membrane systems (Sablani et al., 2001; Valladares Linares et al., 2014). Hydraulics are controlled by the linear flow velocity of the system, which in turn is controlled by factors like thickness and porosity of spacer-filled channel, feed spacer orientation and geometry.

Feed spacers play an important role in spiral-wound membrane systems, by providing inter-membrane space and enhancing mixing. The presence of feed spacers enhances the impact of biofouling on membrane performance (Tran et al., 2007; Van Paassen et al., 1998; Vrouwenvelder et al., 2009a). Research into the modification of feed spacer geometry, either experimentally or by numerical modelling has provided insight into (i) the impact of hydraulics on the performance of spiral-wound membrane systems (Fimbres-Weihs and Wiley, 2010; Koutsou et al., 2007; Madireddi, 1999; Picioreanu et al., 2009; Saeed et al., 2012; Siddiqui et al., 2016; Wiley and Fletcher, 2002), (ii) possibilities to reduce the impact of biofouling on membrane performance (Siddiqui et al., 2017), and (iii) possibilities to enable effective cleaning strategies. Modifying feed spacer properties such as thickness, orientation or filament angle affects the porosity of spacer-filled feed channels.

The porosity of a material is a measure for void spaces in a material expressed as the ratio of the volume of voids over the total volume. In the case of spiral-wound membrane systems, the porosity of the feed channel is expressed as the ratio of the volume of the voids over the total spacer volume, varying in value between 0 and 1. For example, a feed spacer porosity of 0.85 means that the spacer volume consists of 15% material and of 85% voids. Traditionally, the porosity of materials is measured using a device, known as the pycnometer, which measures the density of the material based on the displacement of a liquid such as water or mercury. Measurement of weight and density is another method used for porosity determination in spiral-wound membrane systems (Schock and Miquel, 1987). Recently, numerical modelling has also been applied to determine the porosity of spacer-filled channels. The feed spacer dimensions are measured in a simplified approach or in detail using microscopy and the porosity of the feed channels is calculated by numerical simulations. A computed tomography (CT) scan is a potential tool to determine the dimensions of feed spacers and in combination with numerical modelling, to determine the porosity of spacer-filled feed channels accurately.

In general, research papers describing experimental studies on feed spacers do not mention the method used for determining the spacer channel porosity and its accuracy. Membrane module manufacturers do not always include the spacer porosity and/or do not mention the applied method for assessing the spacer porosity in membrane module specification sheets. So, (i) porosity data is often not provided and (ii) different methods, other than the pycnometer measurement may have been applied but are not mentioned in papers and specification sheets.

1.2. Relationship between porosity, linear flow velocity and pressure drop

In this paragraph the equations for porosity (Ø), linear flow velocity (v) and pressure drop (Δp) are given and the dependency of the linear velocity and pressure drop on the porosity is described and presented in Fig. 1.

The porosity (Ø) of a spacer-filled feed channel is given by eq. (1)

$$(\varnothing) = 1 - \frac{V_{spacer}}{V_{channel}} = 1 - \frac{V_{spacer}}{w_{ch} \times h_{ch} \times l_{ch}} \quad (1)$$

where V_{spacer} is the volume of feed spacer; $V_{channel}$ is the volume of the feed channel which is a product of the height (h_{ch}) of the channel equal to the height of the spacer (e.g. ~863 μm), the length (l_{ch}) and width (w_{ch}) of the feed channel.

The linear flow velocity (v) is described by eq. (2)

$$v = \frac{Q}{A} = \frac{Q}{w_{ch} \times h_{ch} \times \varnothing} \quad (2)$$

where v is the linear flow velocity in $m \cdot s^{-1}$, Q is the feed flow rate in $L \cdot h^{-1}$, A is the area of the feed channel cross section, which is the product of the channel width (w_{ch}), height (h_{ch}) and the porosity of the flow channel:

Eq. (2) shows that the linear flow velocity is inversely proportional to the porosity.

The pressure drop (Δp) can be derived by eq. (3)

$$\Delta p = \lambda \cdot \rho \cdot \frac{v^2}{2} \cdot \frac{L}{d_h} \quad (3)$$

where λ is the friction coefficient, ρ the specific density, v is the linear velocity; L is the length of the membrane and d_h is the hydraulic diameter. The friction coefficient λ is a function of the Reynolds number (Supplementary material).

Eq. (3) shows that the pressure drop is quadratic dependent on the linear flow velocity. The dependency of the linear velocity and pressure drop on the porosity are presented in Fig. 1. Fig. S1 shows the dependency of the linear flow velocity (A) and pressure drop (B) on the porosity for three spacer thickness of 28, 31 and 34 mil. The same trend is observed for different spacer thicknesses, with the lowest starting value for the spacer with a thickness of 34 mil (Supplementary Fig. S1). The figures underline the relevance of an accurate determination and reporting of spacer-filled flow channel porosity data.

1.3. Objectives of this study

The first objective of this study was to assess and evaluate six methods for the porosity measurement applying a pycnometer

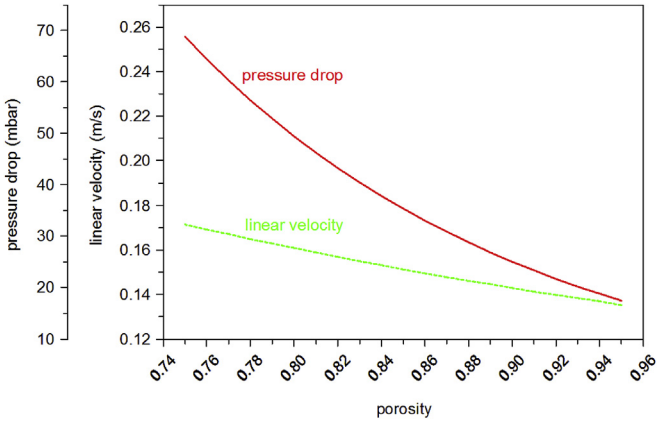

Fig. 1. Linear velocity and pressure drop calculations for a 34-mil (864 μm) thick standard spacer at a feed flow rate of 16 L h^{-1} and a feed channel porosity ranging from 0.75 to 0.95.

(VD), three visually based methods commonly applied for numerical modelling of spacer-filled channels, (simplified (SC) and detailed microscopic methods (VCC and VCE)), weight and density (WD) and X-ray computed tomography (CT) scanning (Table 1). The second objective of this study was to assess and evaluate the impact of the flow channel porosity on the linear flow velocity and pressure drop for the six feed spacers. The six spacers (five of 34 mil and one reference of 31 mil thickness) were placed in membrane fouling simulators (MFSs) to determine the relationship between feed flow and pressure drop. The impact of a deviation in the porosity determination on the actual value of linear velocity and pressure drop was elucidated. To the authors' knowledge, this is the first study addressing the accuracy and relevance of accurate flow-channel porosity measurements for developing spiral-wound membrane modules with improved performance.

2. Materials and methods

2.1. Feed spacers

Six feed spacers with standard and modified geometries were used for this study (Fig. 2). Three spacers coded CON-1, CON-2 and CON-3 (Fig. 2 A–C) were commercially available from Conwed Plastics (Conwed Plastics, Minneapolis, USA). Three modified spacers were produced using a conventional method of spacer manufacturing: a feed spacer from DOW (Fig. 2 D), from Hydranautics coded HYD (Fig. 2 E), and from Lanxess (LANXESS, Bitterfeld, Germany, Fig. 2 F). All spacers consisted of polypropylene material. The thickness of the spacers was 34 mil (863 μm) except for CON-3 with 31 mil (787 μm) thickness.

2.2. Techniques for porosity measurement of spacer-filled feed channels

To determine the porosity of spacer-filled feed channels in membrane based water filtration systems, six different techniques were applied (Table 1).

2.2.1. Microscopic volume measurement methods

The porosity of the spacer-filled channels using microscopic volume methods was determined by measuring the filament thickness or fibre width of the spacer, with the help of stereomicroscopic images (Supplementary Fig. S2) and the number of filament strands (strand count) per meter. Since the feed spacer strand shape is not well defined, the strand volume was calculated assuming cuboidal, cylindrical and ellipsoidal strand shapes as described in the following sections A, B and C:

A. Strand count and fibre volume measurement assuming a cuboidal strand shape (SC): Four samples of each spacer type were taken and five to six measurements were carried out for each sample. The porosity of the spacers was calculated (Supplementary Table S1) assuming a cuboidal strand shape, using eqs. (1) and (4)–(6):

$$V_{strand} = h_f \times w_f \times l_f \tag{4}$$

where V_{strand} is the volume of the spacer strand. h_f is the height of the spacer filament, w_f is the width of the spacer filament and l_f is the fibre length of 1 m (eq. (4)).

The spacer sheet volume (V_{spacer}) was calculated by multiplying the volume of one strand with the strand count (SC) along the fibre length of 1 m (eq. (5)). The volume of the feed channel ($V_{channel}$) is the product of the channel height (h_{ch}) equal to spacer filament height h_f (e.g. ~863 μm), the length (l_{ch}) and the width (w_{ch}) of the channel (1 m each in this case) (eq. (6)).

$$V_{spacer} = V_{strand} \times SC \tag{5}$$

$$V_{channel} = h_{ch} \times l_{ch} \times w_{ch} \tag{6}$$

The porosity was calculated using eq. (1).

B. Strand count and fibre volume measurement assuming a cylindrical shape (VCC): Four samples of each spacer type were taken and five to six measurements were carried out for each sample. The volume of one strand was determined by eq. (7) assuming cylindrical strands (Supplementary Table S2).

$$V_{strand} = \pi \times r^2 \times l_f \tag{7}$$

where r is half of the fibre diameter and l_f is the fibre length (1 m). The volume of the entire spacer sheet (V_{spacer}) was calculated by multiplying the volume of one strand (V_{strand}) with the strand count (SC) along the length of the fibre (eq. (4)). The volume of the feed channel ($V_{channel}$) is the product of the channel height (h_{ch}) equal to spacer filament height h_f (e.g. ~863 μm), the length (l_{ch}) and the width (w_{ch}) of the channel (1 m each in this case) (eq. (6)). The porosity was calculated using eq. (1).

C. Strand count and fibre volume measurement assuming an ellipsoidal strand shape (VCE): In this method, the porosity of spacer-filled feed channels was calculated using the same microscopic volume measurement technique. However, in this method the spacer strand volume was calculated assuming an ellipsoidal instead of a cylindrical structure (Supplementary Table S3) (eq. (8)).

$$V_{strand} = \pi \times r \times \left(h_f / 4\right) \times l_f \tag{8}$$

where r is half of the fibre thickness, l_f is the fibre length (1 m) and h_f the height of the spacer (e.g. ~863 μm). Eqs. (1), (5), (6) and (8) were used to calculate the porosity of spacer-filled channels.

2.2.2. Computed tomographic scan and numerical modelling (CT)

Feed spacer geometries were scanned in small sheets containing six to thirty mesh elements. All feed spacers (coded CON-1, CON-2, CON-3, HYD, DOW and LXS-ASD) were CT scanned with a resolution of 10 μm. The point clouds obtained from the CT scanning

Table 1
Techniques for measuring porosity of spacer filled feed channels.

no.	approach	abbreviation	equipment used	materials and methods section	Table (supplementary)	Figures (supplementary)
1	strand count and fibre thickness	SC	microscope, calliper	2.2.1 A	1	2
2	microscopic volume measurements cylindrical	VCC	microscope	2.2.1 B	2	
3	microscopic volume measurements ellipsoidal	VCE	microscope	2.2.1 C	3	
4	3D CT scan	CT	CT-scan	2.2.2	4	3, 5
5	volume displacement	VD	pycnometer	2.2.3	5	
6	weight and density	WD	scale	2.2.4	6	

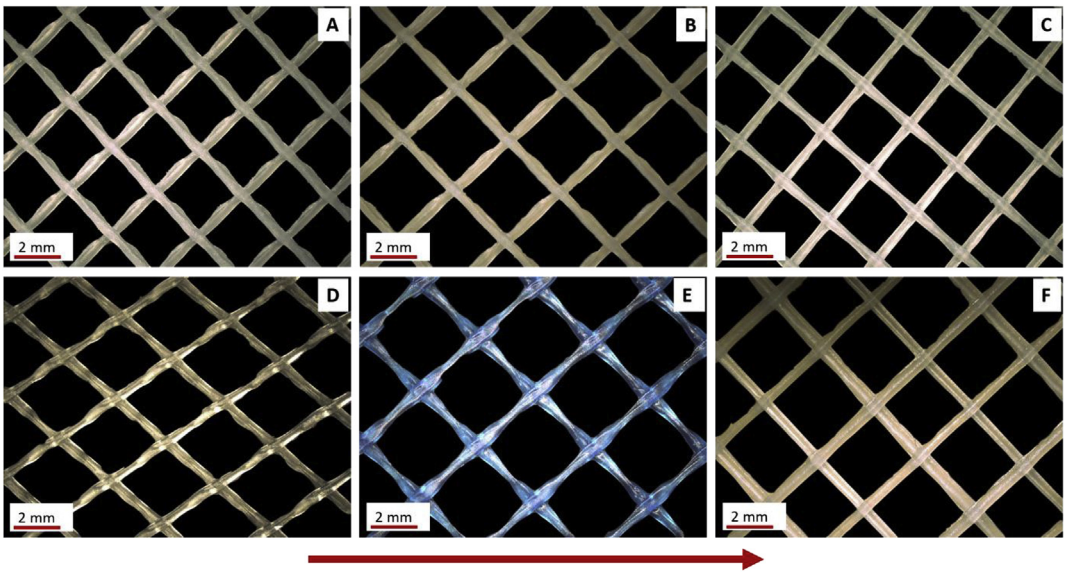

Fig. 2. Microscopic images of six feed spacer types (A) CON-1, (B) CON-2, (C) CON-3 (31 mil), (D) DOW, (E) HYD and (F) LXS-ASD made with a digital camera. Arrow indicates the flow direction.

process were obtained in the STL format (Stereolithography). Prior to using the point cloud for thickness calculations, the feed spacer sheet was trimmed to the desired size using the free version of netfabb, small clusters of vertices resulting from scatter were removed using the open-source tool MeshLab and the resulting point cloud was subsequently exported to a JSON format. Calculations were performed using MATLAB (MathWorks Inc.). Solid geometries (three-dimensional (3D) spacer volume representation) were received in SLDPRT format (SolidWorks Part) created from the point clouds using freeform surface modelling were obtained from CONWED and processed using the interface between MATLAB and COMSOL (COMSOL Inc.) (Supplementary Fig. S3). The porosity measurements for each spacer are provided in Supplementary Table S4.

2.2.3. Volume displacement measurement (VD)

A 500 mL flask was used as a pycnometer and was weighed empty (m_{fl}) and filled with demi water (m_{fl+H_2O}) at T = 22 °C ($m_{H_2O} = m_{fl+H_2O} - m_{fl}$). A spacer coupon was weighed (m_{SP}), placed into the 500 mL flask after which the flask was filled with water until all specimen were covered with water. Attached air bubbles, if any, were removed by air suction for 3 times during 5 min each and by ultrasonification during 30 min. The flask was filled with water to the 500 mL mark and weighed ($m_{fl} + H_2O + SP$, T = 22 °C) (eq. (9)).

$$m_{H_2O+SP} = m_{fl+H_2O+SP} - m_{fl} \tag{9}$$

The volume of the channel ($V_{channel}$) was calculated by eq. (6).

The spacer volume (V_{spacer}) is the volume of water displaced from the flask by adding the spacer. In other words, V_{spacer} is the difference in the water volume before (V_{H2O}) and after adding the spacer coupon (V_{H_2O+SP}) which can be written as follows (eqs. (10) and (11)):

$$V_{spacer} = V_{H_2O} - V_{H_2O+SP} \tag{10}$$

$$V_{spacer} = \frac{m_{H_2O}}{\rho_{H_2O}} - \frac{(m_{H_2O+SP} - m_{SP})}{\rho_{H_2O}} \tag{11}$$

where m_{H_2O} and m_{H_2O+SP} are the weight of the water before and after adding the spacer, m_{sp} is the weight of the spacer and ρ_{H_2O} is the water density.

From the calculated volumes (V_{spacer}, $V_{channel}$) the porosity was calculated by eq. (1) (Supplementary Table S5).

2.2.4. Weight and density measurement (WD)

The porosity was calculated by determining the weight (m_{SP}) of spacer by weighing five 40 mm × 200 mm spacer coupons. The density of the spacer material (ρ_{spacer}) was taken as 0.91 g cm^{-3} (polypropylene from practice).

$V_{channel}$ was calculated by eq. (6).

The density of the channel ($\rho_{channel}$) was calculated by eq. (12).

$$\rho_{channel} = \frac{m_{sp}}{V_{channel}} \tag{12}$$

The porosity was calculated by eq. (13):

$$Porosity(\varnothing) = 1 - \frac{\rho_{channel}}{\rho_{spacer}} \tag{13}$$

The calculated porosities for the six spacers are provided in Supplementary Table S6.

2.3. Experimental setup

The experimental set up (Supplementary Fig. S4) consisted of cartridge filters (pore size of 10 μm) to remove particulate matter, a temperature controller, pressure dampener, digital manometers, pressure reducers, flow controller (mini CORI-FLOW Bronkhorst), differential pressure sensor (Deltabar, Endress + Hauser PMD75, Germany) (Vrouwenvelder et al., 2009b), back pressure valve (Hydra cell, Wanner Engineering Inc., USA), and membrane fouling simulator (MFS).

The MFS has shown to be representative for the hydrodynamics, spatial dimensions and biofouling development of spiral-wound membrane modules (Vrouwenvelder et al., 2007, 2006). The MFS with external dimensions of 0.07 m × 0.30 m × 0.04 m was used in a laboratory set-up under controlled stable conditions to study hydrodynamics, spatial dimensions, and biofouling development (Bucs et al., 2015). Coupons of a virgin membrane and feed spacer of 0.04 m × 0.20 m were placed in the simulator in the same

orientation as in spiral-wound membrane modules in practice. The RO membranes were provided by Trisep Corporation, USA. Experiments were performed with tap water without residual disinfectant.

The hydraulic characterization of the feed spacers was carried out in MFSs by measuring the pressure drop at flow rates, ranging from 0 L h^{-1} to 20 L h^{-1}: equivalent to linear flow velocities of 0.0 m s^{-1} to 0.18 m s^{-1}.

3. Results

Six techniques for porosity measurement were evaluated for three feed spacers with standard and three feed spacers with modified geometries. The feed spacers were first compared with respect to geometry (Section 3.1). Then the results of the various techniques for porosity measurement of spacer-filled feed channels were compared for the six feed spacers (Section 3.2). Finally, the impact of the porosity of the spacer-filled feed channel on the hydraulic behaviour was elucidated (Section 3.3).

3.1. Feed spacer characterization

A visual comparison of the six feed spacers (Fig. 2) was made using a digital microscope (Dino-lite). The feed spacers were characterized based on mesh-size, angle between the filaments and filament thickness of the spacers (section 2.1). Three spacers coded CON-1, CON-2 and CON-3 (Fig. 2 A–C) were commercially available from Conwed Plastics (Conwed Plastics, Minneapolis, USA). Three modified spacers were produced using a conventional method of spacer manufacturing, with slight variations in filament angle, mesh-size and filament thickness: (i) a feed spacer from DOW with an internal strand angle of 70° (Fig. 2 D), (ii) a feed spacer from Hydranautics coded HYD, consisting of 90° internal strand angle and elliptical in cross-section, but with thinner regions between strand intersections and a larger mesh size (Fig. 2 E), (iii) a feed spacer LSX-ASD from Lanxess (LANXESS, Bitterfeld, Germany) with alternating thick and thin strands (Fig. 2 F). CT scan images show the feed spacer top view and cross sections (Fig. 3) and the spacers under a 45° angle (Fig. S5).

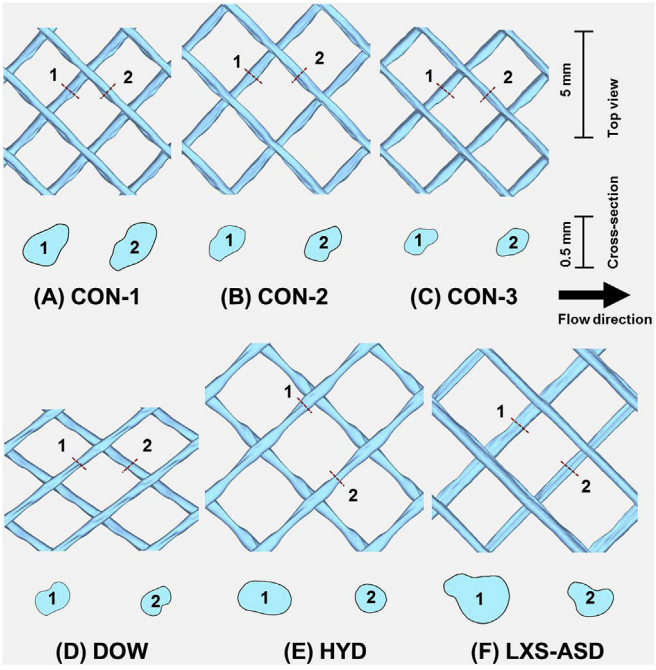

Fig. 3. CT scans of the evaluated feed spacer designs. The top views show the spacers in the xy-plane. Two cross-sections normal to the strand axis (90°), at positions along the strands indicated by dashed red lines, are shown below each top view. All images are presented at the same scale (scale bar for top views, 5 mm; for cross-sections, 0.5 mm). The acronyms refer to the spacer manufacturer: Conwed (CON-1, CON-2, CON-3), DOW (DOW), Hydranautics (HYD) and LANXESS (LXS-ASD). Based on Haaksman et al., 2017. (For interpretation of the references to colour in this figure legend, the reader is referred to the web version of this article.)

3.2. Comparison of measurement techniques for porosity of spacer-filled channels

Fig. 4 and Table S7 show the porosity of spacer-filled feed channels in spiral-wound membrane systems for the six spacers measured by the various techniques. The weight and density (WD) and CT scan (CT) methods showed similar results as the traditional volume displacement (VD) method with a pycnometer, while microscopic measurement techniques: strand count and volumetric calculation (SC, VCC, VCE) showed deviating values with a larger standard deviation. VCE measurements were closer to VD measurements than SC and VCC, which may be due to an ellipsoidal instead of a cuboidal or cylindrical strand shape. The microscopic volume calculation methods had larger standard deviations (Supplementary Table S8). To summarize, compared to the traditional VD method, the microscopic methods SC, VCC and VCE showed strongly deviating values and a larger standard deviation than the WD and CT methods for measuring the porosity of spacer-filled feed channels in spiral-wound membrane systems. Depending on the applied technique the porosity varied between 0.793 and 0.906 with standard variations varying between 0.2% and 6.4% (see Supplementary Tables S7 and S8).

3.3. Impact of the deviation of the porosity on linear flow velocity and pressure drop of spacer-filled feed channels

In section 1.2 the relationship between porosity, linear flow velocity and pressure drop has been discussed. The flow velocity is linear dependent on the porosity while the pressure drop is superlinear dependent on the porosity.

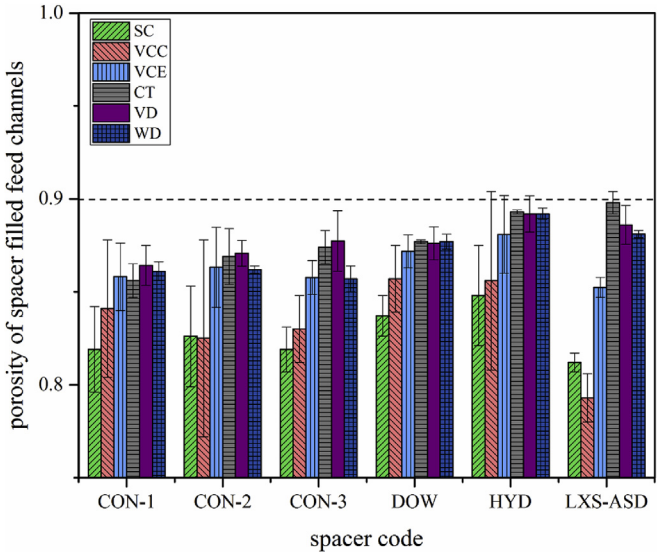

Fig. 4. Comparison of porosities of spacer filled feed channels in MFS for six feed spacers based on porosity methods: volumetric calculations: strand count (SC), cylindrical (VCC) and ellipsoidal (VCE), CT-scan (CT), volume displacement (VD) and weight and density (WD).

In section 3.2 the porosity measurements by six different techniques have been described. For an average porosity value of 0.8 the deviation was about 6%.

Fig. 5 shows the effect of the channel porosity measurement deviation in percent (%) on the linear flow velocity and pressure drop for a 34-mil thick standard spacer at the same feed flow rate.

Fig. 5 shows a significant impact of the deviation of the measured porosity on the linear velocity and especially the pressure drop. For the maximum porosity deviation of −6% to +6%, the deviation of the linear velocity was −5.6% and +6.4% respectively. For the pressure drop the deviations were −31% and +43% respectively, illustrating the importance of an accurate porosity measurement.

3.4. Impact of the porosity on the hydraulic behaviour of spacer-filled feed channels

The hydraulic behaviour of each feed spacer was characterized in MFS research by determining the pressure drop at different flow rates. For each feed spacer, a different relationship between pressure drop and flow rate was observed due to the difference in geometries (Fig. 6).

Once again, deviations in porosity had a strong impact on the relationship between pressure drop and flow rate. Taken the VD measurement as a reference, the deviations in porosity were used to calculate a percentage deviation in pressure drop (see Fig. 7).

The pressure drop deviation varied between −3% for the CT method and +10% for the SC method, once again illustrating the importance of an accurate porosity measurement. Despite the inaccuracy, the impact of the porosity on the hydraulic behaviour of spacer-filled channels has been clearly illustrated.

4. Discussion

The objective of this study was to evaluate the accuracy of six different techniques for measuring the porosity of spacer-filled feed channels in spiral-wound membrane systems and the consequence of an inaccurate porosity method on the performance parameters of spiral-wound membrane systems.

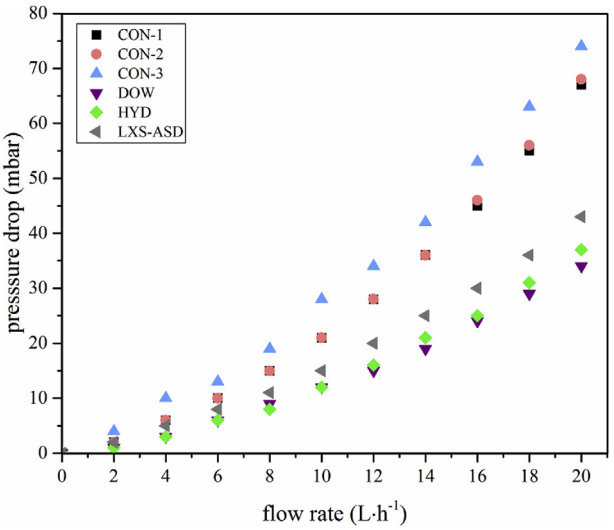

Fig. 6. Feed channel pressure drop (mbar) as a function of feed water flow ($L \cdot h^{-1}$) in MFSs for six different feed spacers: CON-1, CON-2, CON-3, DOW, HYD and LXS-ASD.

4.1. Importance of reporting the porosity of spacer-filled feed channels

Bartels et al. compared spiral-wound membrane modules differing in spacer thickness (26, 28, 31 and 34 mil thick) and design (Bartels et al., 2008). Irrespective of the feed spacer thickness, the membrane modules had the same total membrane surface area (400 sq.ft.) due to a more effective control of glue line placement as well as some other element design changes (Bartels et al., 2008).

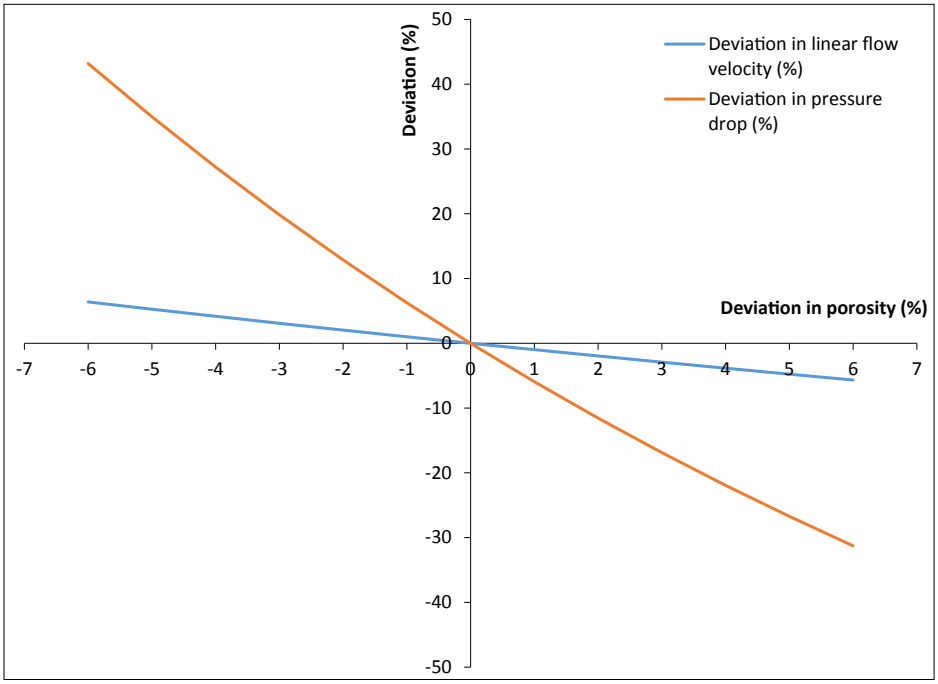

Fig. 5. Effect of feed channel porosity measurement deviation in percent (%) on linear flow velocity and pressure drop for a 34-mil thick standard spacer at a feed flow rate of 16 L h^{-1}.

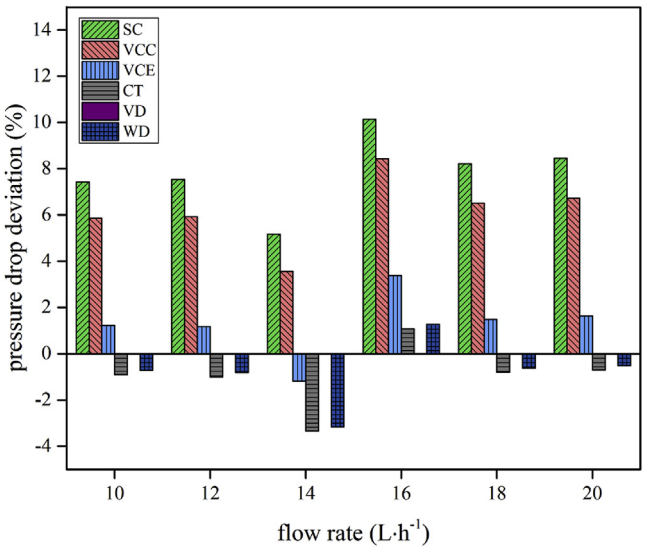

Fig. 7. Effect of different spacer porosity measurements on hydrodynamics for spacer HYD: The percentage differences in porosities can be translated into percentage deviation in pressure drop, with VD as reference method.

The modules containing various feed spacers were tested (i) for the relationship between feed flow rate and pressure drop and (ii) in a pilot study applying the same feed flow rate for the membrane modules while monitoring the pressure drop development. Bartels et al. reported the development of a thicker feed spacer with a unique geometry, a lower pressure drop and a reduced chemical cleaning frequency when treating water of poor feed quality (Bartels et al., 2008). The flow channel porosity was not reported in the study, although the lower pressure drop and the lower pressure drop increase could very well predominantly be caused by the flow channel porosity, instead of the modified spacer design. 55 journal papers were published in the last three years dealing with feed spacers in spiral-wound NF and RO membrane systems. Only eight papers reported the porosity of spacer-filled channels, while only one article mentioned the method used to measure the spacer porosity. To effectively determine the hydrodynamics of the membrane modules, applying a modified feed spacer design, porosity data and method should be reported.

4.2. Applicable methods to measure feed channel porosity

In this study six techniques were applied to measure the porosity of spacer-filled channels as described in section 2.2. The porosity values measured by VD, WD and CT methods were in agreement. The VD method is a simple and accurate method that uses a pycnometer for volume measurements; the only limitations are air bubbles that might distort the volume measurement causing a standard deviation of approximately 1% for all spacer types (Supplementary Table S8). WD is one of the earliest (Schock and Miquel, 1987) and most precise methods with a standard error of <1% (Supplementary Table S8), but accurate density data of the feed spacer are required which may not always be available. The CT method, introduced as an alternative to compare the accuracy of existing methods in practice, proved to be accurate for all spacer types with a percent standard deviation of around 1.0–1.7%. The only limitation of CT is that its accuracy depends heavily on the resolution of the scans.

In the three microscopic techniques, the number of strands per unit area and width of the strands were measured, while assuming the shape of the spacer strand as cuboidal, cylindrical and ellipsoidal for SC, VCC and VCE respectively. The SC and VCC method deviated significantly from the VD method, while the VCE method gave more accurate results, most probably caused by the applied ellipsoidal strand shape.

For spacer coded CON-2 (Supplementary Table S8), the calculated percent standard deviations for SC, VCC and VCE were 3.3%, 6.4% and 2.5% respectively, while for CT, VD and WD the calculated percent standard deviations were 1.7%, 0.8% and 0.2% respectively. In conclusion, VD, WD and CT methods are feasible for measuring the spacer-filled feed channel porosity, while the microscopic methods are shown to be inaccurate and should not be used.

4.3. Effect of porosity measurements on the hydraulics of spiral-wound membrane options and the impact of accumulated biomass

The porosities of the six feed spacers determined by different methods were compared in detail in section 3.2 (see Fig. 4). Following that, the impact of the deviation of the porosity on the linear flow velocity and pressure drop was described in section 3.3. The deviation of the porosity had a strong impact on the linear flow velocity and especially the pressure drop (see Fig. 5). Finally, the impact of the porosity on the hydraulic behaviour of spacer-filled feed channels was explored in section 3.4. Deviations in porosity had a strong impact on the relationship between pressure drop and flow rate. The DOW feed spacer showed the lowest pressure drop flow rate ratio, which may be due to the reduced internal strand angle (β) of 70° (see Fig. 6). CON-2 and DOW had almost the same porosity as indicated by CT data (Fig. 4), but were very different in pressure drop/flow rate ratio (Fig. 6), indicating that the spacer geometry had an influence on hydraulics in addition to porosity. Finally, the effect of the accumulated biomass on the hydraulic behaviour of spacer-filled channels was also strongly impacted by the porosity (Bucs et al., 2014).

The deviation in pressure drop caused by the application of the six different porosity methods was evaluated for spacer coded HYD. Compared to the VD method, the pressure drop variation was as high as 10% for the SC method and as low as 3% for the CT method (see Fig. 7). Therefore, small variations in the porosity led to a significant error in the linear flow velocity and a much larger error in the pressure drop.

4.4. Recommendation

The porosity of spacer-filled channels is important in determining the hydraulics of spiral-wound membrane systems. In literature, the most commonly applied method to determine performance decline is measuring the pressure drop increase over the feed channel. By increasing the porosity of spacers, the pressure drop increase can be reduced significantly, regardless of the amount of fouling present. Some modified membrane modules display an overall reduction in pressure drop due to the higher porosity and not because of a better geometry (Bartels et al., 2008). As shown in this study, both spacer geometry and porosity influence the hydraulic behaviour in spacer-filled channels. To specify the cause of the observed pressure drop reduction, (i) the porosity, (ii) the geometry of the spacer-filled channels should be specified for the spacers used and also (iii) the technique used for calculating the porosity of the spacer-filled feed channels should be mentioned.

5. Conclusions

Comparison of different techniques for porosity measurement of spacer-filled channels using modified feed spacers led to the following conclusions:

- (i) Volume displacement, (ii) CT, and (iii) weight and density based methods have shown to be accurately measuring the porosity of feed spacers.
- Microscopic measurement based methods provide an incorrect porosity of spacer-filled feed channels.
- The porosity of spacer-filled feed channels has a strong impact on linear velocity and pressure drop.
- The linear velocity is proportional and the pressure drop is superlinear (more than proportional) dependent on the porosity.
- Accurate porosity data are essential for the evaluation of feed spacer performance in spiral-wound membrane systems.

Acknowledgement

The research reported in this publication was supported by funding from King Abdullah University of Science and Technology.

Appendix A. Supplementary data

Supplementary data related to this article can be found at http://dx.doi.org/10.1016/j.watres.2017.04.034.

References

Al Ashhab, A., Gillor, O., Herzberg, M., 2014. Biofouling of reverse-osmosis membranes under different shear rates during tertiary wastewater desalination: microbial community composition. Water Res. 67, 86–95. http://dx.doi.org/10.1016/j.watres.2014.09.007.

Baker, J.S., Dudley, L.Y., 1998. Biofouling in membrane systems - a review. Desalination 118, 81–90. http://dx.doi.org/10.1016/S0011-9164(98)00091-5.

Bartels, C., Hirose, M., Fujioka, H., 2008. Performance advancement in the spiral wound RO/NF element design. Desalination 221, 207–214. http://dx.doi.org/10.1016/j.desal.2007.01.077.

Ben-Sasson, M., Zodrow, K.R., Genggeng, Q., Kang, Y., Giannelis, E.P., Elimelech, M., 2014. Surface functionalization of thin-film composite membranes with copper nanoparticles for antimicrobial surface properties. Environ. Sci. Technol. 48, 384–393. http://dx.doi.org/10.1021/es404232s.

Bucs, S.S., Farhat, N., Siddiqui, A., Valladares Linares, R., Radu, A., Kruithof, J.C., Vrouwenvelder, J.S., 2015. Development of a setup to enable stable and accurate flow conditions for membrane biofouling studies. Desalin. Water Treat. 1–9. http://dx.doi.org/10.1080/19443994.2015.1057037.

Bucs, S.S., Radu, A.I., Lavric, V., Vrouwenvelder, J.S., Picioreanu, C., 2014. Effect of different commercial feed spacers on biofouling of reverse osmosis membrane systems: a numerical study. Desalination 343, 26–37. http://dx.doi.org/10.1016/j.desal.2013.11.007.

Fimbres-Weihs, G.A., Wiley, D.E., 2010. Review of 3D CFD modeling of flow and mass transfer in narrow spacer-filled channels in membrane modules. Chem. Eng. Process. Process Intensif. 49, 759–781. http://dx.doi.org/10.1016/j.cep.2010.01.007.

Flemming, H.-C., 2002. Biofouling in water systems—cases, causes and countermeasures. Appl. Microbiol. Biotechnol. 59, 629–640. http://dx.doi.org/10.1007/s00253-002-1066-9.

Haaksman, V.A., Siddiqui, A., Schellenberg, C., Kidwell, J., Vrouwenvelder, J.S., Picioreanu, C., 2017. Characterization of feed spacer channel performance using geometries obtained by X-ray computed tomography. J. Memb. Sci. 522, 124–139. http://dx.doi.org/10.1016/j.memsci.2016.09.005.

Habimana, O., Semião, A.J.C., Casey, E., 2014. The role of cell-surface interactions in bacterial initial adhesion and consequent biofilm formation on nanofiltration/reverse osmosis membranes. J. Memb. Sci. 454, 82–96. http://dx.doi.org/10.1016/j.memsci.2013.11.043.

Koutsou, C.P.P., Yiantsios, S.G.G., Karabelas, A.J.J., 2007. Direct numerical simulation of flow in spacer-filled channels: effect of spacer geometrical characteristics. J. Memb. Sci. 291, 53–69. http://dx.doi.org/10.1016/j.memsci.2006.12.032.

Madireddi, K., 1999. An unsteady-state model to predict concentration polarization in commercial spiral wound membranes. J. Memb. Sci. 157, 13–34. http://dx.doi.org/10.1016/S0376-7388(98)00340-8.

Picioreanu, C., Vrouwenvelder, J.S., van Loosdrecht, M.C.M., 2009. Three-dimensional modeling of biofouling and fluid dynamics in feed spacer channels of membrane devices. J. Memb. Sci. 345, 340–354. http://dx.doi.org/10.1016/j.memsci.2009.09.024.

Ridgway, H.F., Flemming, H.-C., 1996. Membrane Biofouling. McGraw-Hill, New York.

Ridgway, H.F., Kelly, A., Justice, C., Olson, B.H., 1983. Microbial fouling of reverse-osmosis membranes used in advanced wastewater treatment technology: chemical, bacteriological, and ultrastructural analyses. Appl. Environ. Microbiol. 45, 1066–1084.

Sablani, S., Goosen, M.F., Al-Belushi, R., Wilf, M., 2001. Concentration polarization in ultrafiltration and reverse osmosis: a critical review. Desalination 141, 269–289. http://dx.doi.org/10.1016/S0011-9164(01)85005-0.

Saeed, A., Vuthaluru, R., Yang, Y., Vuthaluru, H.B., 2012. Effect of feed spacer arrangement on flow dynamics through spacer filled membranes. Desalination 285, 163–169. http://dx.doi.org/10.1016/j.desal.2011.09.050.

Schneider, R., Ferreira, L., Binder, P., Bejarano, E., Goes, K., Slongo, E., Machafo, C., Rosa, G., 2005. Dynamics of organic carbon and of bacterial populations in a conventional pretreatment train of a reverse osmosis unit experiencing severe biofouling. J. Memb. Sci. 266, 18–29. http://dx.doi.org/10.1016/j.memsci.2005.05.006.

Schock, G., Miquel, A., 1987. Mass transfer and pressure loss in spiral wound modules. Desalination 64, 339–352. http://dx.doi.org/10.1016/0011-9164(87)90107-X.

Schwinge, J., Neal, P.R., Wiley, D.E., Fletcher, D.F., Fane, A.G., 2004. Spiral wound modules and spacers: review and analysis. J. Memb. Sci. http://dx.doi.org/10.1016/j.memsci.2003.09.031.

Siddiqui, A., Farhat, N., Bucs, S.S., Linares, R.V., Picioreanu, C., Kruithof, J.C., Van Loosdrecht, M.C.M., Kidwell, J., Vrouwenvelder, J.S., 2016. Development and characterization of 3D-printed feed spacers for spiral wound membrane systems. Water Res. 91, 55–67. http://dx.doi.org/10.1016/j.watres.2015.12.052.

Siddiqui, A., Lehmann, S., Bucs, S.S., Fresquet, M., Fel, L., Prest, E.I.E.C., Ogier, J., Schellenberg, C., van Loosdrecht, M.C.M., Kruithof, J.C., Vrouwenvelder, J.S., 2017. Predicting the impact of feed spacer modification on biofouling by hydraulic characterization and biofouling studies in membrane fouling simulators. Water Res. 110 http://dx.doi.org/10.1016/j.watres.2016.12.034.

Tasaka, K., Katsura, T., Iwahori, H., Kamiyama, Y., 1994. Analysis of RO elements operated at more than 80 plants in Japan. Desalination 96, 259–272. http://dx.doi.org/10.1016/0011-9164(94)85177-8.

Tran, T., Bolto, B., Gray, S., Hoang, M., Ostarcevic, E., 2007. An autopsy study of a fouled reverse osmosis membrane element used in a brackish water treatment plant. Water Res. 41, 3915–3923. http://dx.doi.org/10.1016/j.watres.2007.06.008.

Valladares Linares, R., Bucs, S.S., Li, Z., AbuGhdeeb, M., Amy, G., Vrouwenvelder, J.S., 2014. Impact of spacer thickness on biofouling in forward osmosis. Water Res. 57, 223–233. http://dx.doi.org/10.1016/j.watres.2014.03.046.

Van Paassen, J.A.M., Kruithof, J.C., Bakker, S.M., Kegel, F.S., 1998. Integrated multi-objective membrane systems for surface water treatment: pre-treatment of nanofiltration by riverbank filtration and conventional ground water treatment. Desalination 118, 239–248. http://dx.doi.org/10.1016/S0011-9164(98)00137-4.

Vrouwenvelder, J.S., Bakker, S.M., Cauchard, M., Le Grand, R., Apacandie, M., Idrissi, M., Lagrave, S., Wessels, L.P., van Paassen, J.A.M., Kruithof, J.C., van Loosdrecht, M.C.M., 2007. The membrane fouling simulator: a suitable tool for prediction and characterisation of membrane fouling. Water Sci. Technol. 197–205. http://dx.doi.org/10.2166/wst.2007.259.

Vrouwenvelder, J.S., Graf von der Schulenburg, D.A.A., Kruithof, J.C.C., Johns, M.L.L., van Loosdrecht, M.C.M.C.M., 2009a. Biofouling of spiral-wound nanofiltration and reverse osmosis membranes: a feed spacer problem. Water Res. 43, 583–594. http://dx.doi.org/10.1016/j.watres.2008.11.019.

Vrouwenvelder, J.S., Manolarakis, S.A., van der Hoek, J.P., van Paassen, J.A.M., van der Meer, W.G.J., van Agtmaal, J.M.C., Prummel, H.D.M., Kruithof, J.C., van Loosdrecht, M.C.M., 2008. Quantitative biofouling diagnosis in full scale nanofiltration and reverse osmosis installations. Water Res. 42, 4856–4868. http://dx.doi.org/10.1016/j.watres.2008.09.002.

Vrouwenvelder, J.S., Van der Kooij, D., 2001. Diagnosis, prediction and prevention of biofouling of NF and RO membranes. Desalination 139, 65–71. http://dx.doi.org/10.1016/S0011-9164(01)00295-8.

Vrouwenvelder, J.S., van Paassen, J.A.M., Kruithof, J.C., van Loosdrecht, M.C.M., 2009b. Sensitive pressure drop measurements of individual lead membrane elements for accurate early biofouling detection. J. Memb. Sci. 338, 92–99. http://dx.doi.org/10.1016/j.memsci.2009.04.016.

Vrouwenvelder, J.S., van Paassen, J.A.M., Wessels, L.P., van Dam, A.F., Bakker, S.M., 2006. The Membrane Fouling Simulator: a practical tool for fouling prediction and control. J. Memb. Sci. 281, 316–324. http://dx.doi.org/10.1016/j.memsci.2006.03.046.

Wiley, D.E., Fletcher, D.F., 2002. Computational fluid dynamics modelling of flow and permeation for pressure-driven membrane processes. Desalination 145, 183–186. http://dx.doi.org/10.1016/S0011-9164(02)00406-X.

Ying, W., Gitis, V., Lee, J., Herzberg, M., 2013. Effects of shear rate on biofouling of reverse osmosis membrane during tertiary wastewater desalination. J. Memb. Sci. 427, 390–398. http://dx.doi.org/10.1016/j.memsci.2012.09.054.